ELSEVIER

Journal of Magnetism and Magnetic Materials 162 (1996) 7–20

journal of magnetism and magnetic materials

Element specific imaging of magnetic domains in multicomponent thin film systems

C.M. Schneider [a,*], K. Meinel [a], J. Kirschner [a], M. Neuber [b], C. Wilde [b], M. Grunze [b], K. Holldack [c], Z. Celinski [d], F. Baudelet [e]

[a] *Max-Planck-Institut für Mikrostrukturphysik, Am Weinberg 2, D-06120 Halle / Saale, Germany*
[b] *Institut für Angew. Physikalische Chemie, Universität Heidelberg, Im Neuenheimer Feld 253, D-69120 Heidelberg, Germany*
[c] *BESSY GmbH, Lentzeallee 100, D-14195 Berlin, Germany*
[d] *University of Colorado, Colorado Springs, CO 80933-7150, USA*
[e] *Laboratoire de Metallurgie Physique and Science des Matériaux, F-54042 Nancy, Cedex, France*

Received 8 June 1995; revised 5 January 1996

Abstract

We employ a new form of photoemission microscopy to image magnetic domains with both element specificity and surface sensitivity. Its contrast mechanisms are based on magneto-dichroic effects in photo-induced Auger electron emission. The method is especially beneficial to the investigation of magnetic domains in multicomponent thin film structures. We demonstrate the capabilities of this technique for the case of epitaxial Cr/Fe(100) thin film systems. The magnetic domain structures of a monatomic Cr layer on Fe, a Cr wedge on Fe, and a wedge shaped Fe/Cr/Fe sandwich structure are investigated for both elements. An antiferromagnetic alignment of the Cr monolayer to the Fe substrate is directly revealed in the images. Exploiting the angular dependence of the magnetic dichroism, regions of bilinear and biquadratic exchange coupling in the Fe/Cr/Fe sandwich are unequivocally identified.

Keywords: Domain imaging; Magnetic dichroism; Interlayer coupling; Thin films

1. Introduction

Magnetic thin film systems continue to be of growing interest in both storage device technology and basic research [1,2]. They exhibit such fascinating effects as, for example, the oscillatory interlayer exchange coupling in sandwich structures [3–5], or the giant magnetoresistance in multilayers [6,7]. The type of films investigated in basic research are usually selected well-defined model systems, with the emphasis lying on an understanding of the physical mechanisms which cause a certain magnetic behavior. Their structure is purposely kept simple, such as a bi- or trilayer, and only the necessary minimum of different chemical species is involved. The main interest in materials research and technology lies in the optimization of one or several particular magnetic properties. This can often be achieved only by building multilayers which contain alloys or compounds, i.e. a larger number of different chemical elements. In parallel with the chemical complexity of the system grows the need to characterize the mag-

* Corresponding author. Fax: +49-345-5511-223.

PII S0304-8853(96)00048-0

netic contribution of the individual components. The discovery of X-ray magnetic circular dichroism (MCD) [8] marked an important step in the development of suitable analytical procedures [9].

A major challenge in the investigation of such layered systems is the elementally resolved imaging of their magnetic microstructure. Several techniques have been established for magnetic domain imaging, for example, the Kerr microscopy [10,11], scanning electron microscopy with spin polarization analysis (SEMPA) [12], or Lorentz microscopy [13,14], to name but a few. Each of these approaches has its specific virtues and drawbacks. The spatial resolution in Kerr microscopy, for example, is diffraction-limited due to wavelength of the light. This poses a serious problem in the investigation of new generation storage media with lateral bit dimensions significantly smaller than one micrometer. Electron beam based methods are more applicable in this case. SEMPA, however, is a very surface sensitive approach, and thus not very well adapted to the analysis of buried layers. Lorentz microscopy, finally, requires particularly thinned samples, since the deflection of the electron beam due to the Lorentz force occurs while the beam passes through the film. Common to all the above techniques is their lack of ability to separate the individual magnetic contributions of the various chemical components in complex thin film systems. There is some very recent progress in separating the magnetic signals from different materials in a layered system by means of magneto-optical Kerr spectroscopy [15]. Whether or not, however, this concept can also be exploited for magnetic domain imaging purposes remains to be seen.

The recent observations of magnetic dichroism in the photo-induced Auger electron yield and in the emission characteristics of core-level photoelectrons have opened up new possibilities for magnetic domain imaging. Applying circularly or linearly polarized synchrotron radiation in the soft X-ray regime, one observes distinct variations of the intensity of the characteristic electrons with the spatial orientation of the magnetization. Various magneto-dichroic effects have been reported up to now: Magnetic circular dichroism (MCD) in the total electron yield [16], MCD in Auger electron emission [17] (both related to an optical excitation at the absorption edges), magnetic circular dichroism in angular resolved core level photoemission (MCDAD) [18], and magnetic linear dichroism in angular resolved core level photoemission (MLDAD) [19,20]. It is important to point out that the above magneto-dichroic phenomena fall into two classes as a consequence of their particular angular dependencies. The absolute magnitude of a magnetic circular dichroism in total or partial electron yield depends only on the angle between the magnetization and the photon spin (or equivalently, the photon wave vector). In contrast, the sign and magnitude of a magnetic dichroism in the angular distribution (MCDAD, MLDAD) varies sensitively with the wave vector of the emitted electron, too. The latter effects can therefore only be discerned with an appropriate angular resolution. Although in principle both classes of magnetic dichroism can be used for magnetic imaging purposes, the difference in the angular dependencies dictates the choice of an appropriate electron-optical column and experimental geometry. In general, employed in conjunction with a spatially resolved analysis of the photocurrent, magnetic dichroism allows an element specific imaging of magnetic domains. In such a magnetically sensitive photoemission microscope domains with a different magnetization show up as regions of different brightness. Elemental selectivity is attained by (i) optical excitation of the electrons at the specific absorption edges and/or by (ii) registration of element characteristic electrons such as Auger electrons or core level photoelectrons.

Two different attempts have been made in order to exploit magneto-dichroic effects for magnetic domain imaging: (i) Photoemission microscopy performed by an immersion lens photoemission microscope (PEEM) as demonstrated by Stöhr et al. [21] and (ii) angular resolved spectro-microscopy employing an imaging electron spectrometer [17,22]. These two approaches involve different electron-optical concepts, which limit the range of kinetic energies of the electrons that form the image. A photoemission microscopy based on the immersion lens concept (PEEM) collects almost all electrons emitted from the sample due to the strong acceleration potentials. Because of this angular integration, the magnetic contrast can only arise from MCD in the total electron yield. The low transmission of the instrument for high-energy electrons, however, finally results in an effective low-pass behavior. The

image is thus predominantly generated by the low-energy secondary electrons. The electron-optics of a spectro-microscopy experiment is constructed with emphasis on the spectroscopy aspect, i.e. with a high transmission over a wide range of kinetic energies. Such an instrument is therefore specially adapted to employ magneto-dichroic effects in the emission of electrons at higher kinetic energy, i.e. Auger electrons and core level photoelectrons, respectively. In addition, only electrons emitted into a small solid angle are used to form the image. The method is therefore not limited to a contrast mechanism based on the angle-integrating MCD, but can in principle exploit MDAD effects as well [23]. A drawback of the spectro-microscopy technique is its presently rather moderate spatial resolution of ~ 1 μm, whereas PEEM-type instruments routinely achieve values well below 1 μm.

The selective use of Auger electrons and core level photoelectrons in spectro-microscopy has two main advantages in comparison to conventional photoemission microscopy. First, one gains improved element specificity as Auger electrons and core level photoelectrons are practically background free. Moreover, in the case of Auger emission the element specificity of Auger electrons can be combined with the element selectivity of the excitation process at the absorption edges. Second, one gains sensitivity to the near surface region due to the relatively small escape depths of the Auger electrons and core level photoelectrons, respectively. By selecting electrons of different kinetic energy, the escape depth may even be varied over a certain range. The surface sensitivity is an essential prerequisite for studying ultrathin magnetic film structures. Given its present limits of the spatial resolution, the combination of element and surface sensitivity is the essential merit of spectro-microscopy. This is important in the investigation of ultrathin films where Kerr microscopy is hampered by a poor signal-to-noise ratio.

In previous experiments, spectro-microscopy has been applied to determine the magnetic domain patterns at the surface of single-crystalline Fe samples [17,22,23] and in layers of rare earth materials on Fe [24]. The investigations were based on MCD in Auger electron emission and core level photoemission. In the present work we demonstrate the potentials of the technique with respect to the element specific imaging of magnetic domains in complex thin film structures by analyzing epitaxial Cr/Fe thin film systems. We study in detail: (i) Cr monolayers (ML) on Fe(100), (ii) Cr wedges on Fe(100), and (iii) Fe/Cr/Fe(100) sandwich structures with the Cr interlayer being of either homogeneous thickness or having a wedge shape. The investigations exploited MCD in Auger electron emission at the $L_{2,3}$ absorption edges, where the strongest magnetic contrasts are observed.

2. Experimental details

The experiments were performed with a VG Escascope described in detail elsewhere [25]. Briefly, the Escascope is an imaging electron spectrometer combining a hemispherical energy analyzer and an electrostatic input lens system (Fig. 1). It can be used either in a spectroscopic mode as a conventional electron spectrometer, or in an imaging mode. With our instrument, a spatial resolution of about 10 μm has been achieved in the imaging mode. The resolution is mainly determined by the chromatic aberration of the purely electrostatic lens system. An improvement by a factor of 5–10 is expected with the incorporation of magnetic lenses [26]. The Escascope

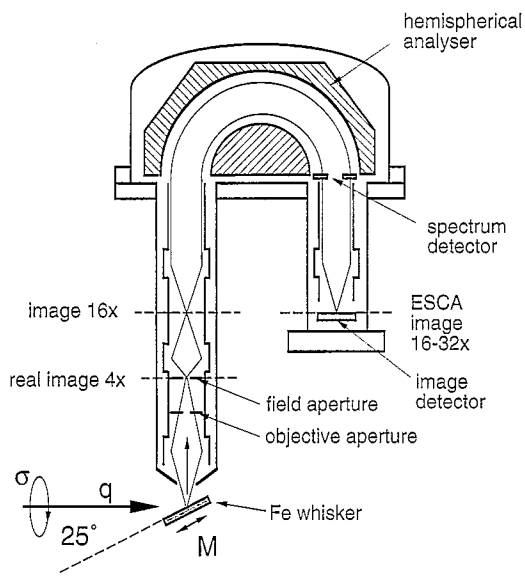

Fig. 1. Schematic diagram of the imaging spectrometer (Escacope) and the experimental geometry.

was installed at the German storage ring BESSY at the SX-700-3 monochromator [27], utilizing the elliptically polarized off-plane radiation. The degree of circular polarization was about 80% at photon energies $h\nu = 600$–800 eV [27].

As templates for the epitaxial growth we used Fe(100) whiskers, onto which Cr and Fe films were deposited. The experiments were performed under UHV conditions (base pressure 1×10^{-10} mbar). The whiskers were cleaned by standard procedures combining Ar^+ ion sputtering and annealing, which yielded almost perfect surfaces with large atomically flat terraces [28]. The Cr and Fe films were grown by molecular beam epitaxy at a rate of about 1 ML/min. During the film deposition the sample temperature was held at about 250°C, where an almost perfect layer-by-layer mode of film growth is established [28–30]. These growth conditions were chosen in order to make contact to previous investigations of the magnetic coupling in the Fe/Cr system [5,28]. Recent results from Auger electron diffraction suggest, however, that although the surface of the growing film stays smooth under these circumstances, the Fe whisker/Cr interface may be subject to some alloying process [31,32]. We will come back to this aspect in the discussion of the results on the magnetism of our structures. The film thickness was determined from the intensities of the Auger electrons and the 2p core level photoelectrons and the corresponding escape depths by assuming exponential attenuation laws [33]. The Cr films were deposited as homogeneous monolayers, or as shallow wedges in order to have a continuous variation of the film thickness. The wedges were prepared by a half shadow technique with a shutter placed between the evaporation source and the sample. In the imaging experiments we took advantage of the regular magnetic domain structure of the whisker substrate. Carefully annealed whiskers usually display in their central part only two major domains of opposite magnetization. The direction of the magnetization points parallel and antiparallel to the whisker axis. The two domains are therefore separated by a 180° domain wall. This simple magnetic domain structure serves as a reliable reference for the interpretation of the magnetic images of the overlayers grown on Fe whiskers.

The magnetic domain imaging was based on the magnetic circular dichroism in Auger electron emission. The effect is closely connected to the well-known magnetic circular dichroism (MCD) in photoabsorption [8]. At the absorption edge the transition probability (or equivalently, the absorption cross section) for the photoexcitation of core electrons into the unoccupied part of the density of states at the Fermi energy depends on the light helicity. During the photoexcitation process a core hole is created, which in turn can decay by means of Auger transitions. Assuming that the Auger process itself does not show an intrinsic magneto-dichroic contribution, the dichroism in the core electron transition probability translates directly into a MCD in the Auger electron yield. Since the high energy Auger electrons are the starting point for a secondary electron cascade, a similar magneto-dichroic signal appears in the total electron yield which is dominated by low-energy secondary electrons. For 3d transition metals the strongest MCD effects are observed in the soft X-ray region at the $L_{2,3}$ absorption edges. The angular dependence of the MCD signal A is simply determined by the relative orientation of photon spin σ and sample magnetization M,

$$A \propto \boldsymbol{\sigma} \cdot \boldsymbol{M}. \tag{1}$$

Since the photon spin of circularly polarized light is either parallel or antiparallel to the photon wavevector q, we can use the angular variation in Eq. (1) to easily determine the spatial direction of the magnetization vector in each magnetic domain. On the one hand, the highest absolute value of the magneto-dichroic signal in Auger emission is observed for parallel or antiparallel alignment of the magnetization vector with respect to the photon beam. On the other hand, the magnetic dichroism disappears for a magnetization vector orthogonal to the light beam. The whisker was therefore mounted on a sample holder which allowed an in-situ rotation about the surface normal. The surface was slightly tilted with respect to the beam, the angle between the photon beam and the whisker surface usually being set to 25°. The emitted electrons were analyzed with the Escascope mounted perpendicular to the photon beam and the storage ring plane (Fig. 1). In most of the experimental runs we used right circularly polarized radiation. The energy of the radiation was tuned to the $L_{2,3}$ absorption edges of Fe (720 and 705 eV)

and Cr (585 and 577 eV), respectively. Simultaneously, the 648 and 529 eV Auger electrons of Fe and Cr, respectively, were registered by the Escascope with an energy resolution of about 2 eV.

Prior to the domain imaging, we first used the instrument in the small spot spectrometer mode in order to find the optimum MCD conditions. The spectroscopic information in this mode stems from a surface area about 100 μm in diameter, and thus permits the determination of the magneto-dichroic signal from a region within a single ferromagnetic domain. The result of this experiment is shown in Fig. 2(a) for the clean Fe whisker substrate, displaying two constant final state spectra $I^{\uparrow\uparrow}$ and $I^{\uparrow\downarrow}$ of the 648 eV Fe Auger electrons. They were measured sequentially from the two oppositely magnetized domains in the central part of the whisker, and reflect the MCD signal for the domain magnetization oriented parallel ($\uparrow\uparrow$) and antiparallel ($\uparrow\downarrow$) to the photon wavevector (Fig. 2a). The magneto-dichroic signal is quantified by the so-called asymmetry function $A(E)$, which is the normalized difference of both measurements

$$A(E) = \frac{I^{\uparrow\uparrow}(E) - I^{\uparrow\downarrow}(E)}{I^{\uparrow\uparrow}(E) + I^{\uparrow\downarrow}(E)}. \tag{2}$$

The asymmetry function reveals two extrema of the MCD signal at the L_2 and L_3 absorption edge of about 15% being opposite in sign (Fig. 2b).

For the purpose of domain imaging this particular spectral dependence of the magneto-dichroic asymmetry turns out to be very useful. Based on Eq. (2), an image which contains only magnetic information can be formed in the following way. In a first step, two Auger electron images $I_3(x,y)$ and $I_2(x,y)$ are taken at the L_3 and L_2 absorption edges. Then the spatial distribution of the magneto-dichroic asymmetry $A(x,y)$, and thus the magnetic image, is calculated as

$$A(x,y) = \frac{I_3(x,y) - I_2(x,y)}{I_3(x,y) + I_2(x,y)}. \tag{3}$$

This procedure has two advantages. First, an enhancement of the magnetic contrast is obtained as the opposite sign of the MCD signal at the $L_{2,3}$ edges leads to a summing up of the absolute values in the intensity asymmetry. Thus the contrast is determined by the full peak-to-peak value of the asymmetry (for Fe almost 30%). Second, other forms of contrast (for example, the topography contrast or the chemical contrast) are eliminated thus facilitating the identification of the magnetic structures. For the Fe whisker this procedure yields a clear bright/dark contrast of the magnetic domains, from which we can easily identify the corresponding directions of the magnetization (Fig. 2c).

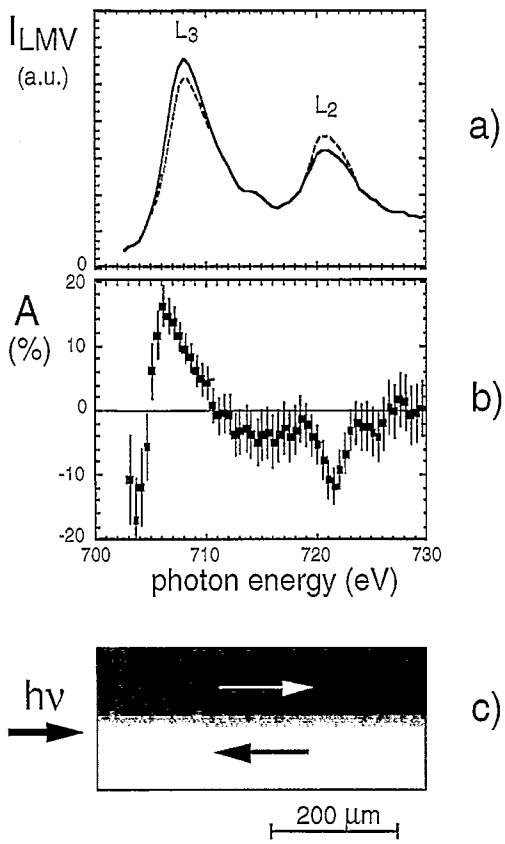

Fig. 2. Magnetic imaging of Fe(100) whiskers using MCD effects in the emission of Fe Auger electrons. (a) Intensity I_{LMV} of the LMV iron Auger electrons (E_{kin} = 648 eV) measured at the $L_{2,3}$ absorption edge with right circularly polarized light for sample magnetization parallel (—) and antiparallel (——) to the photon spin. (b) Corresponding intensity asymmetry A versus photon energy, calculated using Eq. (2). (c) Magnetic domain pattern of a clean Fe(100) whisker surface. The spatial distribution of the peak-to-peak asymmetry is used to generate the contrast.

3. Results and discussion

3.1. Cr / Fe(100) thin film structures

According to the literature [34–38] Cr films on Fe(100) show topological antiferromagnetism consisting of individual atomic layers of ferromagnetic Cr, anti-aligned to adjacent ferromagnetic Cr layers (layered antiferromagnetism). For a ML thick Cr film an antiferromagnetic coupling to the Fe(100) substrate is generally reported.

In Fig. 3(c) we show a magnetic image of a single chromium monolayer grown on the Fe whisker. The noise level in the image is rather high, and is mainly limited by the counting statistics associated with the relatively low intensity of Auger electrons coming from such a thin film. Nevertheless, a magnetic contrast is perceivable. We find the startling result that the contrast is inverted in comparison to the image of the magnetic domains of the clean whisker substrate (Fig. 3b). This becomes more evident when inspecting the behavior in the magneto-dichroic asymmetry in a line scan perpendicular to the domain wall (insets of Fig. 3b,c). The curves represent an average over several vertical line scans taken along the length of the whisker. For the same part of the whisker, the magneto-dichroic signal for chromium has the opposite sign than that for iron. The contrast inversion clearly indicates an antiferromagnetic coupling of the chromium monolayer to the Fe substrate. The asymmetry is relatively low (about 3% peak-to-peak in comparison to the 30% peak-to-peak value of the pure Fe whisker). Idzerda et al. [38] found asymmetry values being greater by almost a factor 3. They studied two-dimensional Cr islands (equivalent of 0.25 ML of Cr layer) by means of MCD in photoabsorption. However, it must be noted that these films were grown at room temperature.

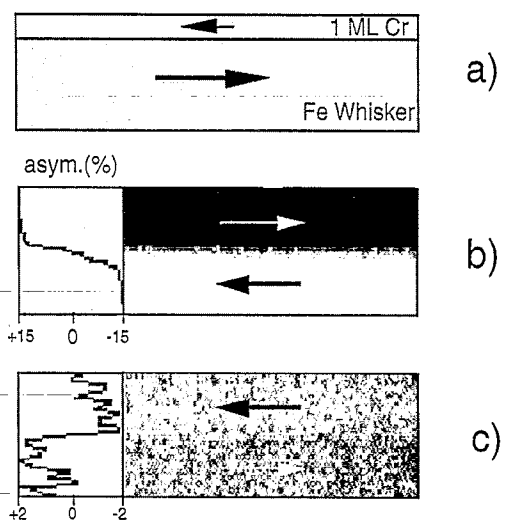

Fig. 3. Magnetic image of 1 ML Cr on Fe(100). (a) Cross section of the film system. (b) Magnetic image of the clean Fe(100) whisker substrate. (c) Magnetic image of the Cr layer obtained with Cr LMV Auger electrons ($E_{kin} = 529$ eV). Insets: Vertical line scans showing the magnitude of the contrast between the two domains with opposite direction of magnetization.

Two mechanisms may be held responsible for the small magneto-dichroic asymmetry observed in our experiment: (i) surface roughness, and (ii) interfacial roughness. In order to see how this will affect the MCD signal, let us first discuss the influence of surface roughness. It is conceivable that our Cr films were not grown in a perfect layer-by-layer mode and displayed already Cr islands in the second layer level. Such a topology would drastically reduce the asymmetry if an antiferromagnetic coupling between neighboring monatomic layers is established within the Cr film. For thicker Cr films a layerwise antiferromagnetic coupling is generally accepted. There is, however, a controversy for ultrathin Cr films. On the one hand, an ideal antiferromagnetic coupling between monatomic Cr layers is presupposed from the very initial stage of the Cr film growth on [35–39]. On the other hand, a magnetic stacking fault has been proposed with the second Cr layer coupling ferromagnetically to the first one [34,36,40]. However, for the latter type of coupling the actual sample topography would have much less influence on the total magnetization and we would observe asymmetry values comparable to that of Izerda et al. [38]. Thus, our results may be more consistent with a magnetic structure based on the ideal antiferromagnetic coupling model for the first few monatomic Cr layers.

We now turn to the question of interfacial roughness. Some theoretical work by Stoeffler and Gauthier [41,42] for non-ideal Fe/Cr interfaces shows a tremendous influence of the interface on the magnetism in the Cr layer. In particular, a chemical intermixing of Fe and Cr at the interface was predicted to change the magnetic moment of the Cr

atoms depending on their local environment [41]. A Cr atom incorporated within the Fe surface (forming the Fe side of the Fe/Cr interface) approximately keeps its magnetic moment and couples antiparallel to the surrounding Fe moments. On the Cr side of the Fe/Cr interface, Cr atoms which are close to this defect have a significantly reduced magnetic moment. In other words, a 'chemical roughening' of the interface which may be caused by atomic exchange processes between the Fe and Cr interfacial layers will diminish the Cr net magnetic moment ('magnetic frustration') and thus the Cr MCD signal. There is some evidence from recent Auger electron diffraction studies that such atomic exchange processes at the Fe/Cr interface do indeed take place at higher growth temperatures [31,32]. At a substrate temperature of about 250°C, as used in the present experiments, about one third of the Cr atoms at the Fe/Cr interface is found on sites within the first iron layer. Assuming the same situation to hold for our samples and taking into account the above arguments by Stoeffler and Gauthier, we thus arrive at an alternative interpretation of our experimental finding: the average magnetic moment in the Cr monolayer is reduced by a certain amount of interfacial alloying between iron and chromium. This still leads to an antiferromagnetic coupling between the Cr monolayer and the Fe substrate but results in a significantly smaller MCD signal than can be expected from a Cr monolayer with a nearly perfect Fe/Cr interface. On the basis of the monolayer results alone it is difficult to decide whether the surface or the interface plays the dominant role in our case. However, considering the results found for thicker Cr films and Fe/Cr/Fe trilayers, we tentatively attribute the small MCD signal of the Cr monolayer to the interfacial alloying rather than to the surface roughness.

In order to study thicker Cr layers we prepared the films in a wedge geometry by means of the half-shadow technique (Fig. 4a). The thickness gradient of the wedges was characterized by a mapping technique using the ratio of the intensities of the Cr and the Fe Auger electrons. For this purpose two Cr images and two Fe images were taken at the corresponding $L_{2,3}$ absorption edges. Then the sum of both Cr images was divided by the sum of both Fe images. In this way the magnetic contrast is eliminated and the resulting image showed a chemical contrast corresponding to the Cr/Fe ratio of the Auger electrons. These mapping technique revealed that the wedges were slightly tilted with respect to the whisker axis due to the deposition geometry. Thus regions of constant thickness are inclined by about 70° relative to the whisker main axis (Fig. 4b). This must be taken into account when interpreting the domain patterns.

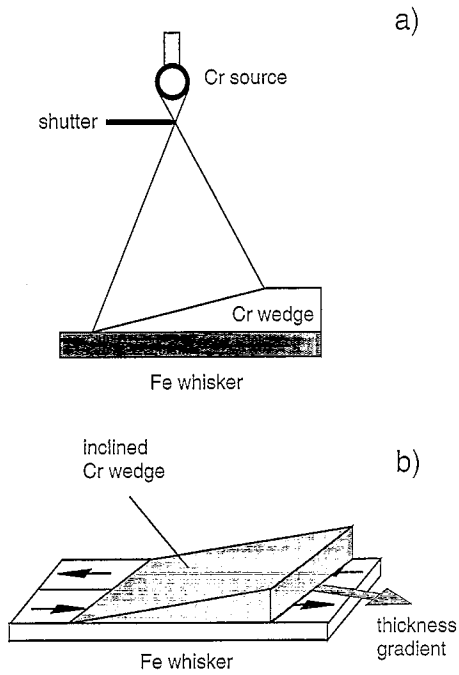

Fig. 4. Preparation of a Cr wedge on Fe(100). (a) Principle of the half-shadow evaporation geometry. (b) Schematic representation of the wedge geometry after chromium deposition. Note the inclination of the thickness gradient with respect to the Fe whisker edge.

The results of the magnetic imaging from a chromium wedge ranging from 3 to 6 ML are shown in Fig. 5. In contrast to the situation in Fig. 3(c), we cannot perceive any magnetic contrast above the statistical noise in the Cr image (Fig. 5b). Even taking into account a moment reduction because of the interfacial alloying, this result is a further indication of the topological antiferromagnetic structure in the chromium layer. Averaged over the thickness of the film the magnetic signal from an individual atomic Cr layer is drastically reduced by the signal of opposite sign from the neighboring layers. The

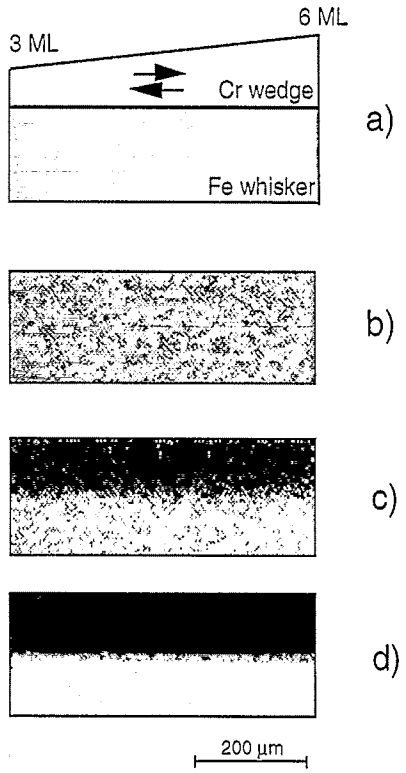

Fig. 5. Magnetic coupling of a Cr wedge on Fe(100). (a) Schematic diagram of the structure. (b) Magnetic image of the Cr wedge. (c) Magnetic image of the Fe whisker seen through the Cr wedge. (d) Magnetic image of the clean Fe whisker surface for comparison.

remaining magnetic signal has obviously dropped below the 1% value of the peak-to-peak asymmetry, which we estimate to be the present sensitivity limit of our method (cf. Fig. 3b). We note that again the data do not support any evidence for a magnetic stacking fault in the second layer. In this case one may expect a small, but sizable domain contrast around 3 ML, which should disappear with a certain gradient towards higher coverages. These findings suggest that the mixed Fe/Cr interface does not only reduce the magnetic moment in the Cr layer, but also effectively suppresses the formation of the magnetic stacking fault found at Cr coverages of 2 ML in room temperature grown films [34,36,40].

Fig. 5(c) shows the image of the Fe whisker obtained with Fe Auger electrons, which have passed through the chromium overlayer wedge. In other words, we are looking through the Cr film onto the Fe substrate. We observe the same magnetic domain pattern as on the clean whisker surface. As one might expect, the magnetic structure in the iron remains unaffected by the Cr overlayer, because it is essentially stabilized by the underlying bulk material. Furthermore, the magnetic contrast in the Fe signal does not vary with the Cr wedge thickness. This is the benefit of the asymmetry formation, which separates the magnetic information and reduces other types of contrast as in the present case the chemical contrast. Note, however, that there is more noise in image 4(c) than in that from the clean whisker surface (Fig. 4d). This noise appears due to the counting statistics and is related to the comparably lower intensity of Fe Auger electrons. The attenuation of the iron signal in the chromium film can in principle be counteracted by increasing the acquisition time for the iron images. This will be necessary, of course, if more complicated domain patterns are investigated.

In addition to the counting statistics, there is an intrinsic effect that leads to a degradation of the image quality. Comparing the magnitude of the magnetic contrast, i.e. the intensity asymmetry, with that of the clean whisker (Fig. 5c,d) we find a distinct contrast reduction for the Cr covered Fe whisker. In the latter case the vertical line scans reveal a peak-to peak asymmetry of only about 20% in comparison to the value of 30% peak-to-peak found in the clean whisker. One might be tempted to attribute this behavior to a reduction of the iron magnetization or even the iron magnetic moment in the presence of the Cr film. If a reduced magnetic signal is obtained with a spatially averaging spectroscopy technique, in which the sample is usually measured in remanence, the origin of a reduced magnetic signal cannot be unambiguously identified. On the one hand, the remanent magnetization along a given spatial direction can always be reduced by the formation of domains. On the other hand, a reduction of the magnetic moment would also lead to a smaller magnetic signal. In the above case of the iron whisker we know from Fig. 5(c), however, that the domain pattern remains unchanged upon chromium deposition. This could point towards a reduced magnetic moment in iron as a possible source of a smaller magnetic dichroism. As discussed in the following, such an interpretation is not necessarily straightforward.

Theoretical investigations predict a clear proxim-

ity effect on the Fe magnetic moment at the Fe/Cr interface [43–46], with the moment reduction itself being of the order of 12–20% as compared to the bulk value of 2.2 μ_B. For the open (001) surface of iron, some 10% enhancement of the surface magnetic moment must be expected. The change of the magnetic moment from a clean Fe surface to the Fe/Cr interface may thus actually be higher. Because of the attenuation of the Fe Auger electrons in the chromium overlayer, the highest contribution to the Fe signal in our experiment comes from the Fe/Cr interfacial region. Taking into account some additional contributions from the adjacent layers, which have essentially the Fe bulk magnetic moment, the corresponding average reduction of the magneto-dichroic asymmetry can be estimated to be certainly less than 10%. This estimate does not yet include possible effects due to the Fe/Cr intermixing at the interface. According to the work of Stoeffler and Gauthier, the magnetic moment of an Fe atom within the Cr interfacial layer is significantly reduced from the bulk value of 2.2 μ_B to about 1.6 μ_B [41]. Assuming for simplicity that the magneto-dichroic signal scales linearly with the magnetic moment, such a moment reduction would bring down the MCD peak-to-peak asymmetry by $\sim 25\%$ as compared to the clean Fe surface. This comes close to the 30% change observed in the experiment. However, we cannot neglects the fact that a significant contribution to the MCD signal comes from Fe atoms within the substrate which should have magnetic moments more or less close to the bulk value. Assuming a reduced magnetic moment of the Fe atoms at the interface is therefore not sufficient to explain the magnitude of the Fe MCD signal. There must be still another mechanism at play.

In order to gain some more information about the origin of the MCD signal, we must examine the particular spectroscopic conditions which apply to the experiment. At the photon energies required for the Fe $L_{2,3}$ absorption (705 and 720 eV) also photoemission from the shallow core levels (3s, 3p) from chromium takes place. The kinetic energy of the Cr 3p photoelectrons exceeds that of the Fe Auger electrons analyzed in the experiment. Consequently, we have a certain background of secondary electrons originating from the Cr 3p transition. These electrons do not carry a magneto-dichroic signal, but contribute to the intensity in both images, and thus tend to reduce the intensity asymmetry, hence the image contrast. In addition, at a photon energy of 720 eV, the Cr 3s photoemission may partially overlap with the Fe 648 eV Auger electron emission. Again, the Cr 3s contribution does not contain magneto-dichroic information, but will reduce the magnitude of the intensity asymmetry. Because of this complicated situation, it is difficult to estimate the overall effect of the Cr photoemission on the magneto-dichroic asymmetry of iron. Further detailed spectroscopic analyses are needed in this case. For the purpose of illustration we may at least estimate the amount of 'non-dichroic' background due to the photoemission from chromium, which is required to reduce the intensity asymmetry of the clean surface to a certain value. In order to explain the above reduction by $\sim 30\%$, one third of the total intensity would have to be Cr-related secondary electrons. In this case, however, one should expect to find a pronounced gradient in the domain contrast of Fig. 4(c), when going from 3 to 6 ML chromium coverage. Such a gradient does not show up in the domain image, indicating that the influence of the Cr-induced background is clearly overestimated in the above example. Taken by itself it cannot explain the observed reduction of the magneto-dichroic signal.

Combining the arguments given above, however, we therefore arrive at the following interpretation. Our experimental finding is compatible with a reduction of the iron magnetic moments at the interface, in accordance with theoretical predictions [41,43,44]. At present, the data do not allow, however, any quantitative determination of the moment reduction. Whether the large reduction of the magneto-dichroic signal may be possibly related to an iron magnetic moment even smaller than predicted by theory, or should to some extend be attributed to a chromium-related background, must be left to future investigations. For this purpose, Fe/Cr systems with different interface morphologies must be studied. Since the interfacial alloying taking place at higher substrate temperatures significantly changes the number of iron and chromium atoms which are in mutual contact, the distribution of Fe and Cr magnetic moments at a sharp interface (which should be obtained with the substrate held at or below room temperature) may be quite different [36].

3.2. Fe / Cr / Fe sandwich structures

Fe/Cr/Fe sandwiches have been one of the first systems, in which an oscillatory interlayer coupling has been observed [3–5]. With increasing thickness of the Cr interlayer the magnetic coupling between the Fe top layer and the Fe substrate alternates between a ferromagnetic (magnetization vectors in film and substrate parallel) and antiferromagnetic (magnetization vectors in film and substrate antiparallel) state. This behavior is often termed as bilinear exchange coupling. In addition, a so-called biquadratic contribution to the exchange coupling is found under particular circumstances [47,48]. Its influence is responsible for a magnetic state of the system in which the magnetization vectors of overlayer and substrate are oriented perpendicular to each other. This state is often referred to as 90° coupling.

We have studied the domain patterns associated with these coupling phenomena for Cr interlayer thicknesses of 0–6 ML where both types of coupling may be found. The chromium interlayer was again grown as a wedge. Since we were mainly interested in the domain pattern of the iron top layer, its thickness was chosen to be about 15 ML. This coverage was high enough to suppress any contributions from the Fe substrate. For the interpretation of the image the reader should keep in mind that lines of constant Cr interlayer thickness are inclined with respect to the whisker axis because of the evaporation geometry. At interlayer thicknesses of 0–4.5 ML we consistently observe the same contrast and domain pattern as for the clean Fe whisker (compare Fig. 5b,c), which indicates that the Fe film is ferromagnetically coupled to the Fe whisker. At chromium interlayer thicknesses of 5–5.5 ML the contrast is reversed, which indicates that the Fe film is antiferromagnetically coupled to the substrate. At Cr interlayer thicknesses of 4.5–5 ML and around 6 ML, however, we do not observe a sizable contrast apart from the statistical noise around the intermediate gray level. This may suggest, among other possible mechanisms, that in these regions the Fe top layer obeys a 90° coupling. Given the particular geometry of the experiment, the magnetization vector of the top layer would be perpendicular to the light beam in this case. According to Eq. (1) the magneto-dichroic signal and consequently also the magnetic contrast will vanish under these conditions. We can therefore generate a contrast in the regions of 90° coupling simply by rotating the sample by an angle of 90°. This brings their magnetization vectors parallel or antiparallel to the photon wave vector and then clear contrasts emerge (Fig. 5d). At the same time the contrast in the ferromagnetically and antiferromagnetically coupled areas must vanish for this geometry. This explains the origin of the regions with a null contrast in Fig. 5(d). By combining the two images in Fig. 5(c,d), we can easily reconstruct the complex magnetic domain pattern of the coupled Fe film in a schematic diagram, which contains both the spatial distribution and orientation of the magnetization (Fig. 5e).

Our results essentially confirm the findings of Unguris et al. [5]. When comparing our images to theirs, however, the different thickness gradient must be taken into account. Whereas in the NIST samples the Cr interlayer thickness varies by 0.1 ML/μm, our samples have been grown with a gradient of 5×10^{-3} ML/μm. Within a comparable field of view, we therefore observe only a small number of periods of the oscillatory coupling and the regions of biquadratic coupling appear rather wide. Expressed in absolute numbers, however, the biquadratic coupling in our films extends laterally over a distance of ~ 120 μm. From Fig. 5(a) and (c) in Ref. [5], we estimate the stripes of biquadratic coupling to be about 8 μm wide. Scaled with our thickness gradient this amounts to a value of ~ 180 μm, which must be compared to our results. From this comparison follows that in our samples the regions of biquadratic coupling in the same range of Cr interlayer thickness are about one-third narrower than those in Ref. [5]. This appears to be the only significant difference in the results. At Cr interlayer thicknesses above 6 ML there is another transition from the biquadratic to antiferromagnetic coupling, as can be deduced from the dark contrast in the right-hand corner of Fig. 6(c). If a ferromagnetic coupling were present at this point we should expect a bright contrast. One is therefore led to the conclusion that the coupling in the region of small interlayer spacing is predominantly of antiferromagnetic character (determined by the long period oscillation), and the short period oscillation in the interlayer exchange coupling shows up only by the formation of regions with biquadratic

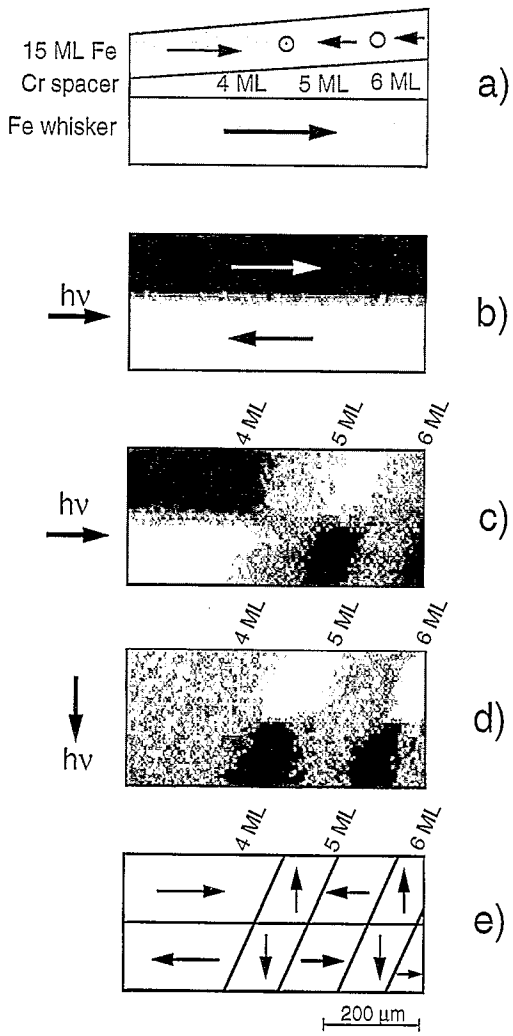

Fig. 6. Magnetic coupling in a wedge shaped Fe/Cr/Fe(100) sandwich system. (a) Cross section of the film system. (b) Image of the Fe whisker substrate prior to the Cr deposition taken with photon spin along the Fe whisker main axis. (c,d) Images of the magnetic domains in the top Fe layer taken with photon spin along (c) and perpendicular (d) to the main whisker axis. (e) Schematic diagram of the main magnetic domains in the top Fe layer.

coupling. This result fully confirms the findings reported by Unguris et al. [5] and Heinrich et al. [28].

At first glance, the domain pattern in the Fe overlayer, particularly in the regions of the 90° coupling, seems energetically unfavorable. A configuration in which two oppositely magnetized domains are facing each other will create a large stray field energy. Apart from a simple minimization principle of the magnetic stray field, however, two other mechanisms have to be taken into account in this sandwich system. First, the domain pattern is mainly determined by the interlayer coupling, and thus not directly comparable to that of a simple surface or a thin film. The magnetic stray field energy may well be overcompensated by the energy gained by the magnetic coupling. In applying the stray field argument for the interpretation of the domain pattern therefore the entire system has to be considered. Second, a close inspection of the domain patterns in Fig. 5(c,d) reveals that the domains are bounded by curved rather than straight lines (as drawn for reasons of simplicity in Fig. 5e). In addition, in a superposition of Fig. 5(c,d) the domain boundaries appear 'decorated' by small regions which do not exhibit a sizable contrast in any of the two directions of light incidence. Recalling that our spatial resolution is of the order of 10 μm, we attribute this behavior to the formation of microdomains with an average size of less than 10 μm. Since we cannot resolve these microdomains in the imaging process, we see only the average over the four possible magnetization directions, being close to a null effect. The formation of microdomains and associated flux closure structures at the domain boundaries and at the whisker edge can effectively reduce the magnetic stray field energy. Clearly, an access to these interesting phenomena requires an improved spatial resolution.

Various approaches have been used to describe the coupling from the viewpoint of theory. There are basically two main concepts: (i) total energy schemes including ab initio calculations [49,50], tight-binding calculations [41,51–54] or quantum well approaches [55–59], and (ii) perturbation models, which are based on theories of the Ruderman–Kittel–Kasuya–Yosida (RKKY) type [60,61]. In addition, significant attempts have been made to develop a unified non-perturbative theory [62–64]. Encouraging results have been obtained in explaining the origin of the ferromagnetic and antiferromagnetic coupling. The origin of the 90° coupling, however, is still a matter of debate. Various models have been proposed, including an intrinsic origin [56,62–69], loose spins [69], and dipole interactions [70]. In addition, the 90°

coupling has been suggested to arise from structural imperfections such as growth roughness [70,71], pin holes [72], and diffuse interfaces due to interdiffusion [70]. Such film imperfections, of course, cannot be completely excluded during film growth. In most cases, one is forced to accept a compromise. Preparing the films at low temperature may suppress interdiffusion but may cause a higher degree of structural disorder and surface/interface roughness. Growing the films at higher temperatures as in our experiments may lead to a perfect layer-by-layer mode of film growth with increased structural perfection, but may at the same time promote interdiffusion or interface alloying. In the present case of the Fe/Cr/Fe sandwiches grown at high substrate temperature, the available results on the magnetism in this system indicate a pronounced effect of the interface on the behavior of the interlayer coupling [31,32], and may point towards interface alloying as a possible origin of the biquadratic coupling. We wish to recall that interdiffusion effects play a particularly important role at low film thicknesses or at the very beginning of film deposition, respectively, because they proceed much faster in ultrathin films than in the bulk due to the diffusion size effect [73]. It would therefore be interesting to investigate the annealing behavior of Cr films on Fe grown at room temperature, in order to see whether sharper Fe/Cr interfaces and a reasonably flat Cr surface can be obtained simultaneously that way. In addition, a certain degree of surface or interface roughness remains even for a perfect layer-by-layer growth, as the growth proceeds in an oscillating manner via the repeated nucleation and coalescence of two-dimensional islands. Thus further experimental and theoretical efforts are required for a complete understanding of the magnetism in sandwich structures. In particular, the correlations of the magnetic coupling to the structural properties of the interfaces must be examined in more detail.

4. Summary and outlook

Magnetic spectro-microscopy based on magneto-dichroic effects in photoelectron and Auger electron emission opens up new possibilities in the investigation of the magnetism in multicomponent thin film systems. It enables the imaging of magnetic domains with element specificity and surface sensitivity. Exploiting magnetic circular dichroism in Auger electron emission we have demonstrated the potentials of this technique by analyzing Cr/Fe thin film systems. The individual domain structures of the Cr and Fe components could be imaged separately even for single monolayer coverages.

Up to now the present approach has two major limitations. First, the spatial resolution of the available spectro-microscopy instruments is relatively poor (10 μm in the case of our instrument, and 1–2 μm in the improved version). Second, the acquisition time is comparably long (almost 1 h for a magnetic image in the case of our experiments on Cr monolayers). These limitations, however, will soon be surpassed by the development of suitable electron-optical imaging systems. In particular PEEM-type instruments have a great potential for improvement in this respect and instruments which routinely achieve a sub-micron lateral resolution will soon be seen in operation [74] The acquisition time can be significantly cut down by using the access to dedicated beamlines at high-brilliance synchrotron radiation sources of the next generation which are currently becoming available.

In future applications, not only magnetic circular dichroism in Auger electron emission may be utilized, but also the various types of magneto-dichroic effects in the emission of core level photoelectrons [18,23], which are also highly element specific. The main advantage of using core level photoelectrons will be the exploitation of magneto-dichroic effects observed with linearly polarized synchrotron radiation [19,20]. Linearly polarized synchrotron radiation with high brilliance is currently more easily available. Such magneto-dichroic effects are in principle observable also with unpolarized radiation generated in conventional laboratory X-ray tubes [75]. Because of reasons of brilliance, however, exploitation of the unpolarized magnetic dichroism with laboratory sources will probably be limited to spectroscopy applications. Electron emission microscopies on the basis of magneto-dichroic phenomena with circularly and linearly polarized light offer a unique access to the magnetism in complex thin films systems, and will soon play an important role in their magnetic characterization.

Acknowledgements

We would like to thank B. Zada for her technical support. One of us (F.B.) would like to express his gratitude to the Alexander von Humboldt Stiftung (AvH Foundation) for supporting his stay by a research fellowship. We acknowledge the hospitality of the Physics Department of the Freie Universität Berlin. The work was supported by the Bundesministerium für Forschung und Technologie (grants No. 055EFAAI5 and No. 055VHFX1).

References

[1] R.F.C. Farrow, B. Dieny, M. Donath, A. Fert, and B.D. Hermsmeier, eds., Magnetism and Structure in Systems of Reduced Dimensions (Plenum Press, New York, 1993).
[2] J.A.C. Bland and B. Heinrich, eds., Ultrathin Magnetic Structures (Springer, New York, 1994).
[3] P. Grünberg, R. Schreiber, Y. Pang, M.B. Brodsky and H. Sowers, Phys. Rev. Lett. 64 (1986) 2442.
[4] S.S.P. Parkin, N. More and K.P. Roche, Phys. Rev. Lett. 64 (1990) 2304.
[5] J. Unguris, R.J. Celotta and D.T. Pierce, Phys. Rev. Lett. 67 (1991) 140.
[6] M.N. Baibich, J.M. Broto, A. Fert, F. Nguyen Van Dau, F. Petroff, P. Eitenne, G. Creuzet, A. Friederich and J. Chazelas, Phys. Rev. Lett. 61 (1988) 2472.
[7] G. Binasch, P. Grünberg, F. Saurenbach and W. Zinn, Phys. Rev. B 39 (1989) 4828.
[8] G. Schütz, W. Wagner, W. Wilhelm, P. Kienle, R. Zeller, R. Frahm and G. Materlik, Phys. Rev. Lett. 58 (1987) 737.
[9] C.T. Chen, Y.U. Idzerda, H.-J. Lin, G. Meigs, A. Chaiken, G.A. Prinz and G.H. Ho, Phys. Rev. B 48 (1993) 642.
[10] J. Kranz and A. Hubert, Z. Angew. Phys. 15 (1963) 220.
[11] F. Schmidt, W. Rave and A. Hubert, IEEE Trans. Magn. 21 (1985) 1596.
[12] H.P. Oepen and J. Kirschner, Scanning Microsc. 5 (1991) 1.
[13] E. Fuchs, Naturwiss. 47 (1960) 392.
[14] J.N. Chapman, J. Phys. D 17 (1984) 623.
[15] G. Pénissard, P. Meyer, J. Ferré and D. Renard, J. Magn. Magn. Mater. 146 (1995) 55.
[16] C.T. Chen, F. Sette, Y. Ma and S. Modesti, Phys. Rev. B 42 (1990) 7262.
[17] C.M. Schneider, K. Meinel, K. Holldack, H.P. Oepen, M. Grunze and J. Kirschner, Mater. Res. Soc. Symp. Proc. 313 (1993) 631.
[18] C.M. Schneider, D. Venus and J. Kirschner, in: Vacuum Ultraviolet Radiation Physics, eds. F. J. Wuilleumier, Y. Petroff and I. Nenner (World Scientific, Singapore, 1992) p. 421.
[19] C. Roth, F.U. Hillebrecht, H.B. Rose and E. Kisker, Phys. Rev. Lett. 70 (1993) 3479.
[20] C. Roth, H.B. Rose, F.U. Hillebrecht and E. Kisker, Solid State Commun. 86 (1993) 647.
[21] J. Stöhr, Y. Wu, M.G. Sarmant, B.D. Hermsmeier, G. Harp, S. Koranda, D. Dunham and B.P. Tonner, Science 259 (1993) 658.
[22] C.M. Schneider, K. Holldack, M. Kinzler, M. Grunze, H.P. Oepen, F. Schäfers, H. Petersen, K. Meinel and J. Kirschner, Appl. Phys. Lett. 63 (1993) 2432.
[23] C.M. Schneider, Z. Celinski, M. Neuber, C. Wilde, M. Grunze, K. Meinel and J. Kirschner, J. Phys.: Condens. Matter 6 (1994) 1177.
[24] T. Kachel, W. Gudat and K. Holldack, Appl. Phys. Lett. 64 (1994) 655.
[25] P. Coxon, J. Krizek, M. Humpherson and I.R.M. Wardell, J. Electron Spectr. and Related Phenemena 51–52 (1990) 821.
[26] The manufacturer reports that the VG ESCALAB 220i, representing the next generation of imaging spectrometers, will achieve a spatial resolution of around 2 μm.
[27] H. Petersen, M. Willmann, F. Schäfers and W. Gudat, Nucl. Instr. and Meth. A 333 (1993) 594.
[28] B. Heinrich, M. From, J.F. Cochran, L.X. Liao, Z. Celinski, C.M. Schneider and K. Myrtle, Mater. Res. Soc. Symp. Proc. 313 (1993) 119.
[29] D.T. Pierce, J.A. Stroscio, J. Unguris and R.J. Celotta, Phys. Rev. B 49 (1994) 14564.
[30] J.A. Stroscio, D.T. Pierce and R.A. Dragoset, Phys. Rev. Lett. 70 (1993) 3615.
[31] B. Heinrich, J.F. Cochran, D. Venus, K. Totland, C.M. Schneider and K. Myrtle, J. Magn. Magn. Mater. 156 (1996) 215.
[32] B. Heinrich, J.F. Cochran, D. Venus, K. Totland, D. Atlan, S. Govorkov and K. Myrtle, J. Appl. Phys. 79 (1996) 4518.
[33] G. Ertl and J. Küppers, Low Energy Electrons and Surface Chemistry (VCH, Weinheim, 1985).
[34] C. Carbone and S.F. Alvarado, Phys. Rev. B 36 (1984) 2433.
[35] R. Jungblut, C. Roth, F.U. Hillebrecht and E. Kisker, J. Appl. Phys. 70 (1991) 5923.
[36] F.U. Hillebrecht, C. Roth, R. Jungblut, E. Kisker and A. Bringer, Europhys. Lett. 19 (1992) 711.
[37] T.G. Walker, A.W. Pang, H. Hopster and S.F. Alvarado, Phys. Rev. Lett. 69 (1992) 1121.
[38] Y.U. Idzerda, L.H. Ljeng, H.-J. Lin, C.J. Gutierrez, G. Meigs and C.T. Chen, Surf. Sci. 287–288 (1993) 741.
[39] P. Fuchs, K. Totland and M. Landolt, in: 14th Int. Colloq. on Magnetic Films and Surfaces (ICMFS), Düsseldorf, 1994.
[40] C. Turtur and G. Bayreuther, Phys. Rev. Lett. 72 (1994) 1557.
[41] D. Stoeffler and F. Gauthier, Phys. Rev. B 44 (1991) 10389.
[42] D. Stoeffler and F. Gauthier, J. Magn. Magn. Mater. 147 (1995) 260.
[43] R.H. Victora and L. M. Falicov, Phys. Rev. B 31 (1985) 7335.
[44] C.L. Fu, A.J. Freeman and T. Oguchi, Phys. Rev. Lett. 54 (1985) 2700.
[45] A. Vega, L.C. Balbas, A. Chouairi, C. Demangeat and H. Dreyssé, Phys. Rev. B 49 (1994) 12797.
[46] I. Mertig, Private communication.

[47] M. Rührig, R. Schäfer, A. Hubert, R. Mosler, J.A. Wolf, S. Demokritov and P. Grünberg, Phys. Status Solidi (a) 125 (1991) 635.
[48] J. Unguris, D.T. Pierce, R.J. Celotta and J.A. Stroscio, in: Magnetism and Structure in Systems of Reduced Dimensions, eds. R.F.C. Farrow, B. Dieny, M. Donath, A. Fert and B.D. Hermsmeier (Plenum Press, New York, 1993).
[49] P.M. Levy, K. Ounandjela, S. Zhang, Y. Wang, C.B. Sommers and A. Fert, J. Appl. Phys. 67 (1991) 5914.
[50] F. Herman, J. Sticht and M. van Schilfgaarde, J. Appl. Phys. 69 (1991) 4783.
[51] H. Hasegawa, Phys. Rev. B 42 (1990) 2368.
[52] H. Hasegawa, Phys. Rev. B 43 (1991) 10803.
[53] D. Stoeffler and F. Gauthier, Prog. Theor. Phys. Suppl. 101 (1990) 139.
[54] D.M. Edwards, J. Mathon, R.B. Muniz and M.S. Phan, J. Phys.: Condens. Matter 3 (1991) 4941.
[55] J. Barnas, J. Magn. Magn. Mater. 111 (1992) L215.
[56] R.P. Erickson, K.B. Hathaway and J.R. Cullen, Phys. Rev. B 47 (1993) 2626.
[57] K.B. Hathaway and J.R. Cullen, J. Magn. Magn. Mater. 104–107 (1991) 1840.
[58] J.R. Cullen and K.B. Hathaway, J. Appl. Phys. 70 (1991) 5879.
[59] M.D. Stiles, Phys. Rev. B 48 (1993) 7238.
[60] Y. Wang, P.M. Levy and J.L. Fry, Phys. Rev. Lett. 65 (1990) 2732.
[61] P. Bruno and C. Chappert, Phys. Rev. Lett. 67 (1991) 1602.
[62] J. Mathon, M. Villeret and D.M. Edwards, J. Magn. Magn. Mater. 127 (1993) L261.
[63] J. Mathon, M. Villeret, J.M. Mander, D.M. Edwards and R.B. Muniz, Mater. Res. Soc. Symp. Proc. 313 (1993) 171.
[64] P. Bruno, J. Magn. Magn. Mater. 121 (1993) 248.
[65] D.M. Edwards, J. Mathon, R.B. Muniz, M. Villeret and J.M. Ward, in: Magnetism and Structure in Systems of Reduced Dimensions (Plenum Press, New York, 1993) p. 401.
[66] D.M. Edwards, J.M. Ward and J. Mathon, J. Magn. Magn. Mater. 126 (1993) 380.
[67] J. Barnas and P. Grünberg, J. Magn. Magn. Mater. 121 (1993) 326.
[68] J. Inoue, J. Magn. Magn. Mater. 136 (1994) 233.
[69] J.C. Slonczewski, J. Magn. Magn. Mater. 126 (1993) 374.
[70] S. Demokritov, E. Tsymbal, P. Grünberg, W. Zinn and I.K. Schuller, Phys. Rev. B 49 (1994) 720.
[71] J.C. Slonczewski, Phys. Rev. Lett. 67 (1991) 3172.
[72] J.F. Bobo, H. Fischer and M. Piecuch, Mater. Res. Soc. Symp. Proc. 313 (1993) 467.
[73] M.G. Goldiner, V.B. Sapoznikov, M. Klaua and K. Meinel, J. Phys.: Condens. Matter 3 (1991) 5479.
[74] Using a photoemission electron microscope magnetic domain imaging with a spatial resolution of ~250 nm and chemical imaging with a spatial resolution of ~40 nm has been reported by E. Bauer's group at the TU Clausthal in a recent BESSY Newsletter (No. 5, July 1995).
[75] F.U. Hillebrecht and W.-D. Herberg, Z. Phys. B: Condens. Matter 93 (1994) 299.